Geological Quarterly, 2007, **51** (4): 375–392

Conodont-based graphic correlation of upper Givetian-Frasnian sections of the Eastern Anti-Atlas (Morocco)

Sofie GOUWY, Joanna HAYDUKIEWICZ and Pierre BULTYNCK

Gouwy S., Haydukiewicz J. and Bultynck P. (2007) — Conodont-based graphic correlation of upper Givetian-Frasnian sections of the Eastern Anti-Atlas (Morocco). Geol. Quart., **51** (4): 375–392. Warszawa.

A high-resolution correlation of ten upper Givetian-Frasnian sections spread over the different facies environments of the Eastern Anti-Atlas (Morocco) is established using graphic correlation. The measured stratigraphic ranges of eighty-five conodont taxa have been assembled into a chronostratigraphic framework. The developed regional composite subdivides the Frasnian into 501 composite standard units (CSU) based on the original thickness of the reference section (Bou Tchrafine). This is a higher resolution than obtained by the classic biozone correlation. Based on the conodont data available for this correlation project, the *jamieae* and Lower *rhenana* zones could not be recognised in the sections.

Sofie Gouwy, Dipartimento di Scienze della Terra, Università di Modena e Reggio Emilia, Largo Santa Eufemia 19, I-41100 Modena, Italy, e-mail: sofiegouwy@yahoo.com; Joanna Haydukiewicz, Instytut Nauk Geologicznych, Uniwersytet Wrocławski, ul. Cybulskiego 30, PL-24-205 Wrocław, Poland, e-mail: jhay@ing.uni.wroc.pl; Pierre Bultynck, Royal Belgian Institute of Natural Sciences, Vautierstraat 29, B-1000 Brussel, Belgium, e-mail: pierre.bultynck@naturalsciences.be (received: May 4, 2007; accepted: November 12, 2007).

Key words: Morocco, Devonian, conodonts, graphic correlation.

INTRODUCTION

In the Eastern Anti-Atlas, upper Givetian-Frasnian conodonts have been studied for decades, cited in stratigraphical studies (e.g., Massa, 1965; Bensaid, 1974; Hollard, 1974; Kaufmann, 1998; Becker and House, 2000) or papers focussing on conodonts (e.g., Müller and Bensaid, 1969; Bultynck and Hollard, 1980; Bultynck and Jacobs, 1981; Bensaid *et al.*, 1985; Bultynck, 1986, 1987; Belka *et al.*, 1999).

The purpose of the present paper is to correlate by the method of graphic correlation several upper Givetian and Frasnian pelagic and more neritic successions from the Tafilalt and the Ma'der. In some successions with a mixed pelagic-neritic facies (El Atrous II) or a neritic facies (Bou Terga and Ammessoui) a correlation based on classic conodont biozones has proved to be difficult because some of the index species are absent. In graphic correlation, however, correlations are based on a composite of the first and last occurrences of all taxa present, not just on the ranges of biozone markers in the various sections. Thus graphic correlations have the potential of greater precision than classical biozone correlations. The Bou Tchrafine section, providing the most complete conodont data among the sections studied herein, is used as Frasnian regional, composite reference section. Some of the field and conodont data used in this work were published before (Bultynck and Hollard, 1980; Bultynck and Jacobs, 1981; Bensaid *et al.*, 1985; Bultynck, 1986, 1987; Becker and House, 2000; Bultynck and Walliser, 2000*a*; Gouwy and Bultynck, 2002). The conodont data, however, have been updated and completed. The study of the Bou Terga, Hamer El Khdad and Hassi Oum El Hadej sections is new.

GEOLOGICAL SETTING

The Anti-Atlas region is an exposed part of the passive continental margin of Northwestern Gondwana. During the Late Devonian, this region was situated in the southern hemisphere at latitudes of about 40° (Scotese, 2004). It constituted a fragment of an extensive shelf area the bathymetry of which started to change during the Early Devonian (late Emsian). As a consequence facies differences became apparent during the Middle Devonian (Eifelian) so that four depositional realms can now

be distinguished in the Eastern Anti-Atlas. From west to east they are: Ma'der Platform, Ma'der Basin, Tafilalt Platform and Tafilalt Basin (Wendt, 1985). This pattern, emphasized by contrasts in facies patterns and subsidence rate, persisted until the Early Carboniferous.

The upper Givetian and Frasnian of the region is predominated by the pelagic facies, but the facies show a significant differentiation. The Frasnian of the Tafilalt belongs to the hemipelagic and pelagic facies, while in some parts of the Ma'der and the southwestern part of the Tafilalt (El Atrous II) transitional facies between pelagic and neritic facies can be observed. At the base of the Frasnian, strongly condensed sequences occur in most parts of the region and there is evidence of non-sedimentation and erosion. In the Frasnian and Famennian deposits, repeated siliciclastic input and sedimentary gaps can be found. These gaps occur at different stratigraphic positions in different areas.

SECTIONS AND CONODONT DATA

The correlated sections are geographically widespread and represent a variety of facies (Fig. 1). Although the sections are remote, the lack of vegetation and beautiful exposure allows for easy sampling.

TAFILALT PLATFORM

This pelagic platform corresponds to a shallow pelagic ridge (Wendt *et al.*, 1984) and is characterized by a succession of strongly condensed cephalopod limestones, nodular limestones and styliolinid coquinas. Six sections of this area are included in the graphic correlations, two of which are situated at the southern margin of the platform (Jbel El Atrous and Jbel Amessoui)

BOU TCHRAFINE (FIG. 2)

Bou Tchrafine is the name of a prominent limestone ridge located about 8 km SE of Erfoud. The Bou Tchrafine upper Givetian-Frasnian succession used in the correlation is a composite section containing data from 4 closely located outcrops: BT I, II and III of Bultynck (1986) and the Bou Tchrafine section described by Becker and House (2000). Section BT I was also studied by Bultynck and Jacobs (1981) and by Bultynck and Hollard (1980). The upper Givetian deposits of this location consist of brownish-pink limestones, unit K Bultynck and Walliser (2000*b*) of the Bouia Formation (Achguig Group). The oldest Frasnian deposits are dark styliolinid coquinas that are recognized in the 4 outcrops although with a different thickness and are followed by marly shales alternating with thick grey limestone beds. The first appearance of black deposits indicates the *semichatovae* transgression (Becker and House,

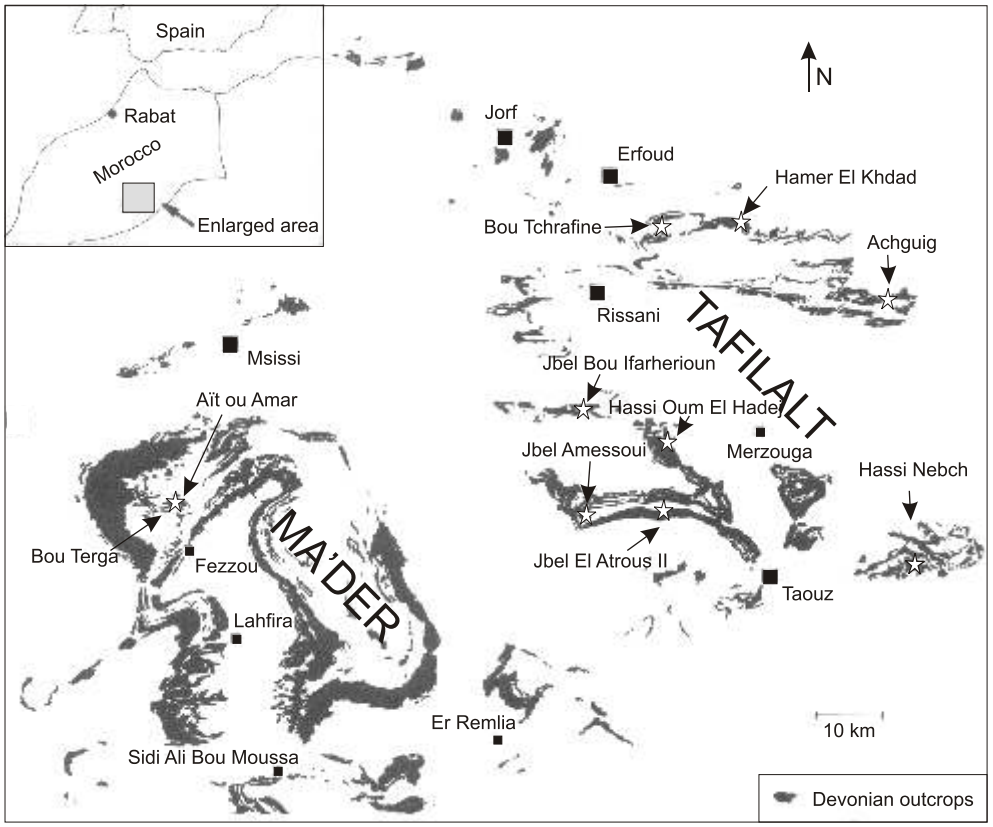

Fig. 1. Location of the sections (asterisks) in the Eastern Anti-Atlas (Morocco)

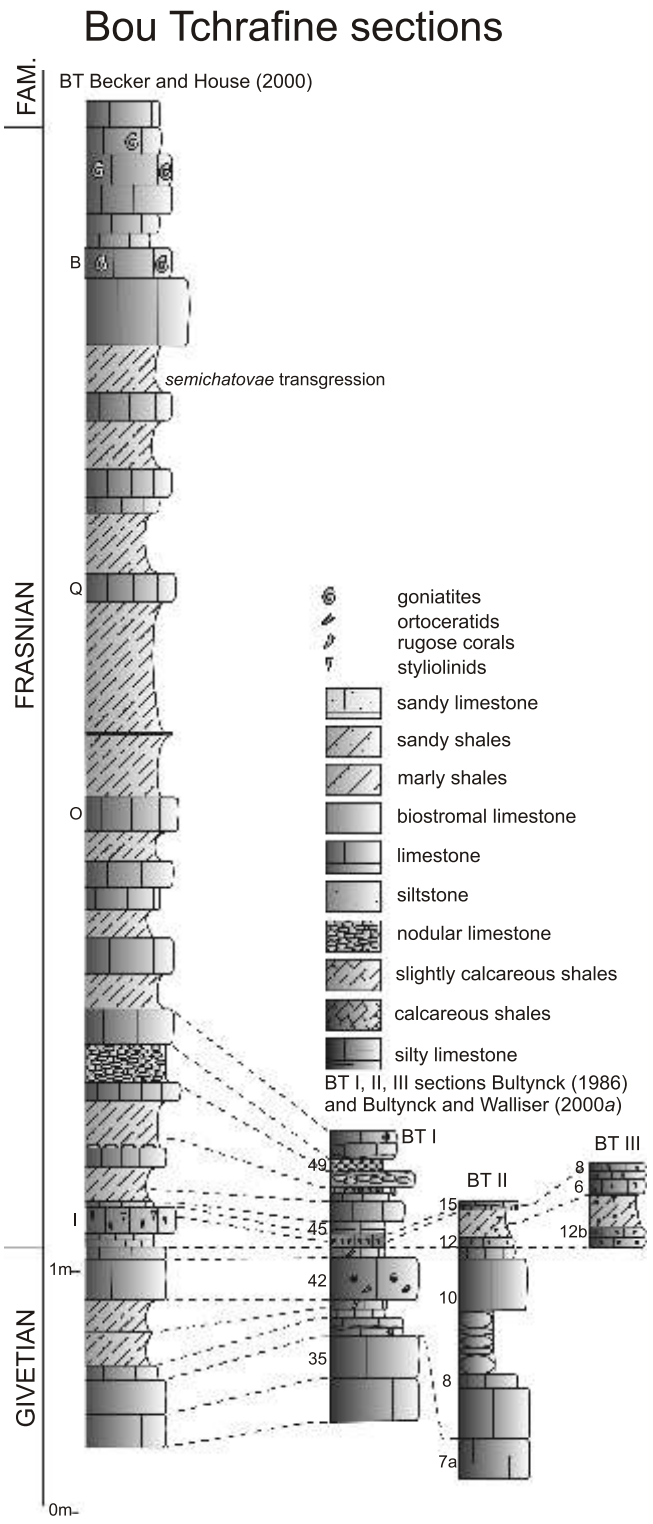

Fig. 2. Set of the Bou Tchrafine reference sections used for building the upper Givetian-Frasnian regional composite reference section of the Tafilalt–Ma'der region

For the complete set of sample numbers see Bultynck (1986, fig. 2), Bultynck and Walliser (2000*a*, fig. 8) and Becker and House (2000, fig. 1); for the ranges of the conodont taxa in composite standard units see the Appendix

2000). The Lower and Upper Kellwasser events are represented by black limestones in the upper part of the section (Becker and House, 2000). Most conodont zones from the *hermanni* to the *linguiformis* zones were recognized.

JBEL EL ATROUS II (FIG. 3A AND B)

The Jbel El Atrous II section is located about 16 km northwest of Taouz, on the southern flank of the El Atrous syncline. The upper Givetian and lower Frasnian deposits are in neritic facies. Biostromal facies with Phillipsastreae occurs (Coen-Aubert, 2002) in the lower part of the section. The upper part of the section consists of marly shales intercalated with thin limestone beds. This section was published by Bensaïd *et al.* (1985) and is completed herein above the sample 23. The samples above the sample 54 were provided by P. Sartenaer. Most conodont zones from the *disparilis* to the Middle *triangularis* zones were recognized.

HAMER EL KHDAD SOUTH (FIG. 4)

This section is situated in a passage track 8 km east of the Bou Tchrafine section and 2 km south-west of the Hamer El Khdad carbonate mound. The section represents a slightly deeper depositional environment than the Bou Tchrafine section and consists of thick limestone beds and nodular limestones rich of macrofossils. Some beds are iron-rich or show signs of erosion. The conodont data indicate a gap in the upper Givetian and the lower Frasnian (the Frasnian begins here in the *punctata* Zone) and at the base of the Famennian where the Lower and Middle *triangularis* Zones are missing.

JBEL BOU IFARHERIOUN

The Ifarherioun section is located at the southern margin of the Tafilalt Platform, 19 km south of Rissani and consists of marly shales locally alternating with nodular limestones and a few massive limestone beds. The uppermost part of the section consists of a massive limestone. Sample 13a is from a well-developed styliolinid coquina facies, which often occurs at the base of the Frasnian in the region (Bensaid *et al*., 1985). Based on the conodont data, the bases of the *disparilis*, *transitans*, *punctata* and Upper *hassi* zones can be positioned.

JBEL AMESSOUI

This section is located 14 km west of the Jbel El Atrous II section. The lithology consists of marly shales and a few decimetre thick limestone beds. The upper part of the section shows a few silty limestone beds. Only the Upper *falsiovalis* and the *transitans* zones can be recognized here. Conodonts of this section were studied by Bensaid *et al.* (1985).

HASSI OUM EL HADEJ

This section is only a few metres thick and is situated about 20 km west of the town of Merzouga and north of the Jbel Amessoui section. The lithology is very similar to the Jbel Amessoui section. It contains a covered interval of about 6 m between deposits of the Upper *falsiovalis* Zone and the

punctata Zone. The lowest bed above the covered interval is a styliolinite. The Lower *hassi* Zone is also recognized.

TAFILALT BASIN

The basin deepens to the east and is for the major part covered by Upper Cretaceous/Quaternary deposits of the Hamada du Guir. Only the western margin of this basin is exposed.

ACHGUIG

This section, located 34 km ESE of Erfoud, was selected as a reference section for the region by Bultynck and Walliser (2000*b*, fig. 5). It is one of the most complete sections in which the entire Devonian is represented, predominantly in a basinal hemipelagic facies. The Frasnian part of the section is composed of marly shales alternating with only a few thin limestone layers. The goniatite bed near the base of the stratigraphic column belongs to the unit K of Bultynck and Walliser (*ibidem*), and is directly overlain by a styliolinite. The *hermanni*, *disparilis* and Lower and Upper *hassi* zones were recognized.

HASSI NEBCH

This section is located about 19 km ENE of Taouz. The upper Givetian-Frasnian is represented by marly shales alternating with thin limestone and nodular limestone beds. A few silty beds occur in the uppermost part of the Givetian. The Frasnian deposits consist of marly shales alternating with fewer and thicker limestone beds and nodular limestone beds (Bensaid, 1972, 1974; Bensaid *et al*., 1985). Of all the sections, this one represents the deepest depositional setting in respect to the pelagic facies of the Tafilalt and is therefore less condensed than the other sections. Conodont zones that can be recognized here are the *disparilis*, Upper *falsiovalis*, *transitans*, *punctata* and the Upper *hassi* zones. However, the conodont material from this section does not allow for exact positioning of the zonal boundaries. *Ancyrognatus* aff. *Anc. triangularis* recognized by Bensaid *et al.* (1985, fig. 5, sample 57) is assigned herein to *Anc. tsiensi* and the identification of *Palmatolepis subrecta* is not maintained.

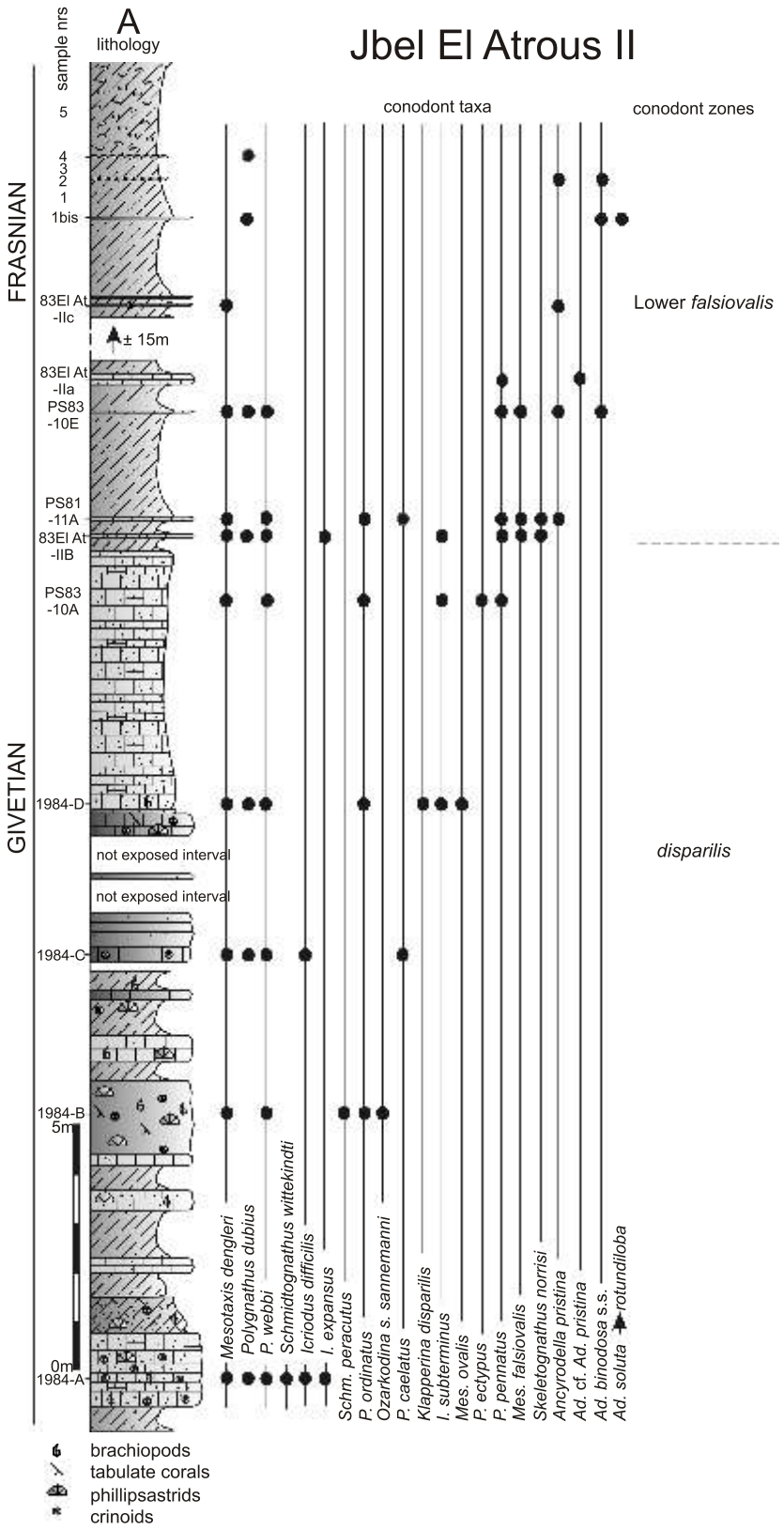

Fig. 3. Stratigraphic column of the Jbel El Atrous II section

A — lower part of the Jbel El Atrous II;

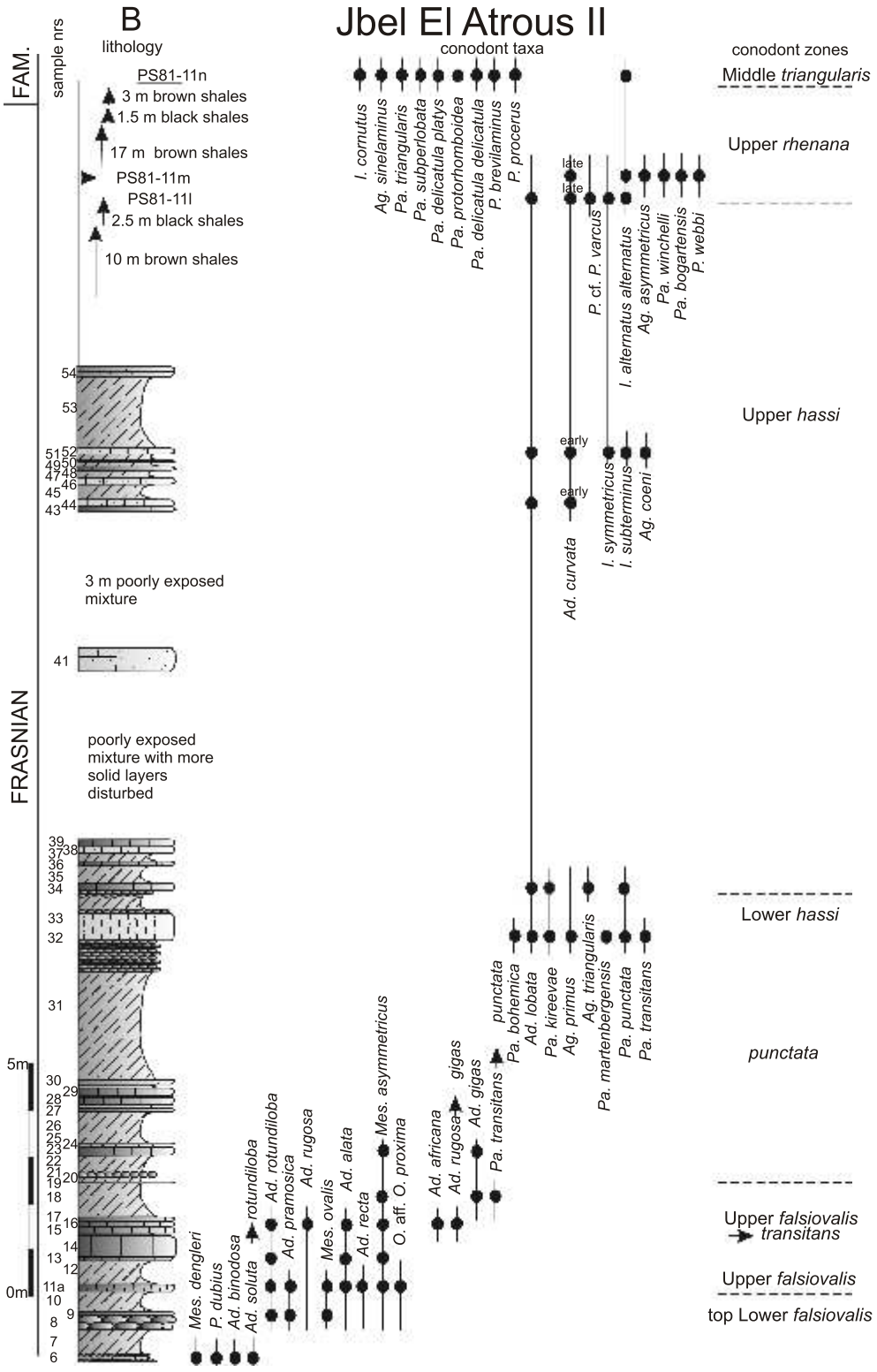

with indication of the conodont taxa per sample and conodont biozonation

B — upper part of the Jbel El Atrous II; lithology as in Figure 2

MA' DER BASIN

This basin is a circular depression with high subsidence rates, which received muddy and fine clastic input from the surrounding partly emerged pelagic platforms and from the eroded hinterland to the west.

BOU TERGA (FIG. 5)

The Bou Terga section is located about 9 km north-west of Fezzou, 2 km west-southwest of of the section "Butte 760" in Bultynck and Jacobs (1981, fig. 1). It consists of about 60 m of marly shales and thin limestone beds, some of which contain goniatites, crinoids and brachiopods. The lower part of the section includes calcareous shales with Phillipsastreae. The Lower *falsiovalis*, *punctata*, Lower *hassi* and Upper *rhenana* zones can be identified, although the bases of the zones cannot be positioned accurately.

AIT OU AMAR

This small section is situated 5 km east of the Bou Terga section and consists of about 0.5 m of thin, biosparitic limestone beds (see Bultynck and Jacobs, 1981, fig. 5). Conodonts indicate that it should be assigned to the *falsiovalis* Zone, based on the occurrence of *Ad. binodosa*, *Ad. pristina* and *Ad. rotundiloba* (Bultynck and Hollard, 1980; Bultynck and Jacobs, 1981).

GRAPHIC CORRELATION METHOD

The graphic correlation method (Shaw, 1964) used herein to correlate several

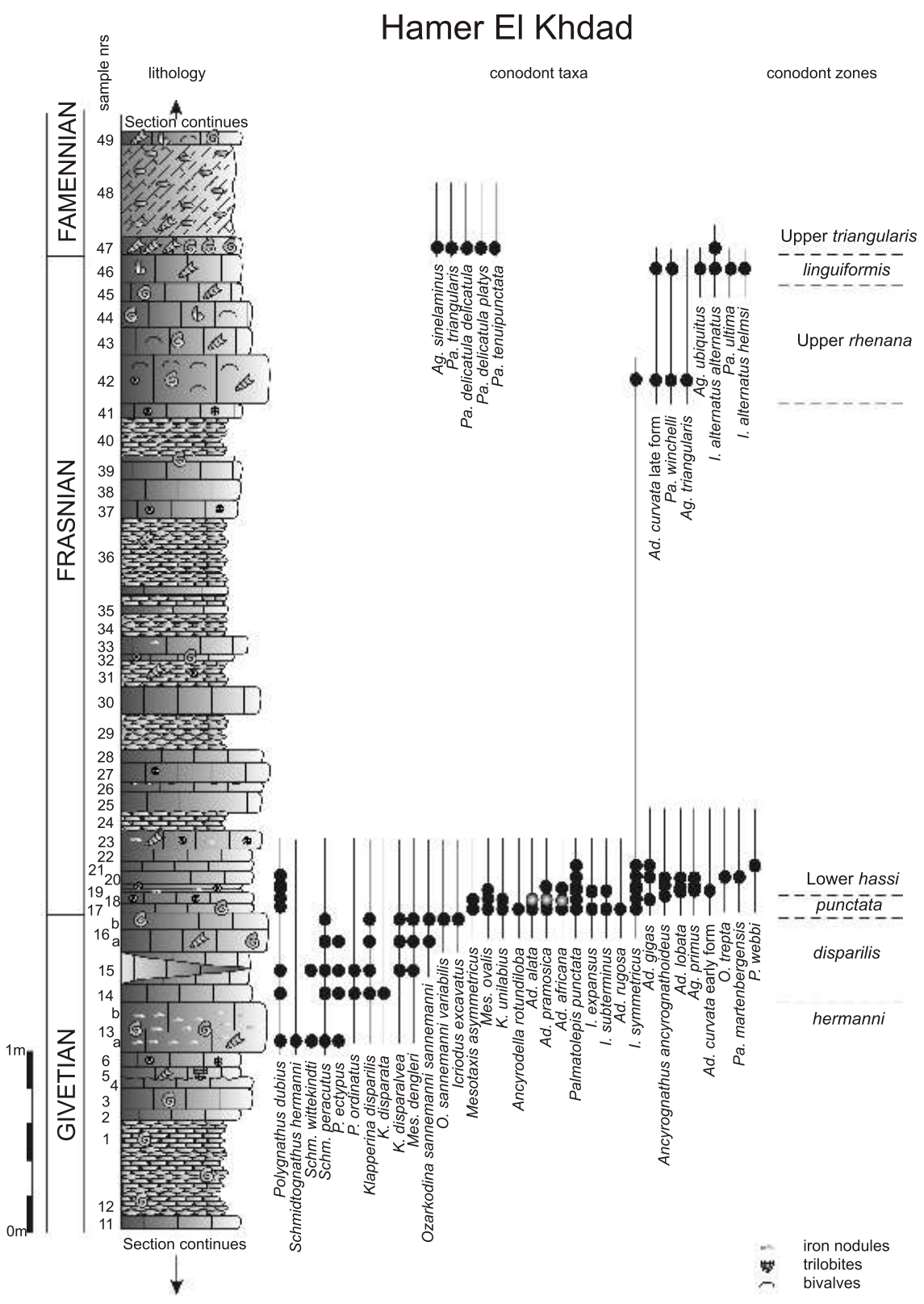

Fig. 4. Stratigraphic column of the Hamer El Khdad South section with indication of the conodont taxa per sample and conodont biozonation

Lithology and faunal symbols as in Figures 2 and 3

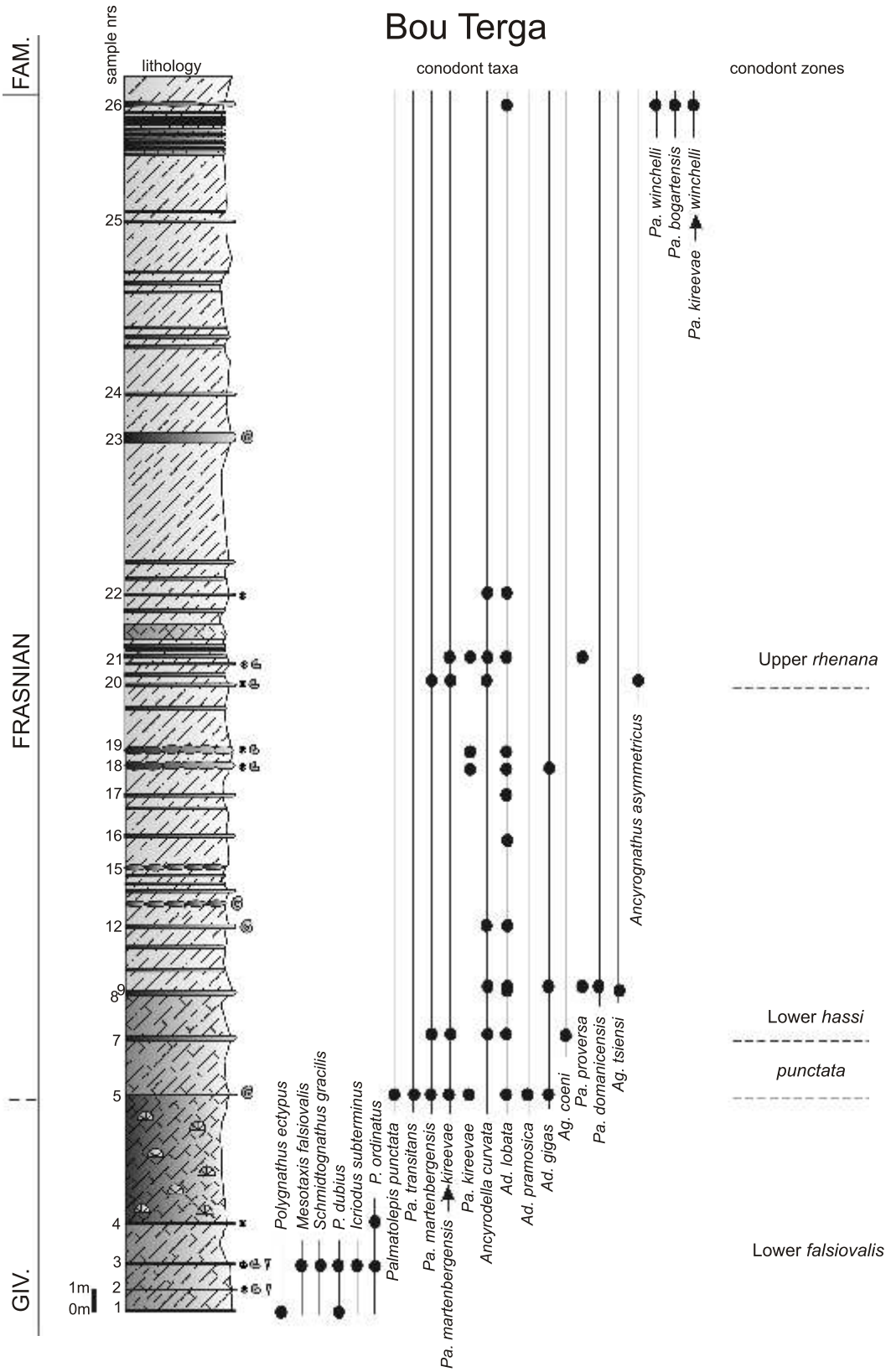

Fig. 5. Stratigraphic column of the Bou Terga section with indication of the conodont taxa per sample and the conodont biozonation

Lithology and faunal symbols as in Figures 2 and 3

time-equivalent sections is a technique based on a Cartesian coordinate system. The sections are correlated by plotting them two-by-two on the axes of an X–Y graph. The thicknesses of the sections are scaled on the axes. One of the sections is chosen as the standard reference section (SRS) to which all other sections of the area will be correlated in the building of a composite sequence of all the sections. The SRS is generally the best-sampled, non-tectonised section with the largest and most varied fossil content and also the thickest one, without important stratigraphic gaps, and containing the youngest and oldest deposits to be studied. The data selected for the correlation should be coeval geologic events so that a one-to-one time correspondence can be established between correlated sections. In this study the events are first and last occurrences of conodont species. Unfortunately, because of factors of sampling density and size, fossil preservation, facies changes, and migration of taxa, such bioevents recorded in given sections are only exceptionally the evolutianary or global first and last occurrences of the species. Even the actual lowest local position may lie at or stratigraphically above the observed one. To take these variables into account, errorboxes are used to bracket the ranges. They indicate the distance between the sample containing the first occurrence of a species and the first sample below that does not contain it and the distance between the sample containing the last occurrence of a species and the first sample above that does not contain the species. The actual first and last occurrence in the section will presumably lie in the errorbox, thus estimating the position of the event. The goal is to improve the estimate.

Each section is correlated with the standard reference section. The fossil data in common between the two sections plot in the field of the graph where the square sign (□) denotes first appearance datum (FAD) while "plus" (+) marks last appearance datum (LAD). The line of correlation representing the point-by-point time-equivalence of the sections is drawn in a way as to cause minimum change of known ranges ("splitting tops and bases"— Klapper *et al.*, 1995). After each correlation round, data from the correlated section are projected onto the standard reference section thus composing a composite section or "composite standard" (CS) for the region. After completing the whole correlation process, this composite standard will contain the maximum ranges of the conodont species for the region.

The scale of the composite standard is subdivided into composite standard units (CSU) based on the original thickness scale of the reference section. These units can be projected onto the other sections through their lines of correlation, the result of which is high-resolution correlation of the sections.

This method has the advantage that time-equivalent sections that previously could not be correlated due to a lack of a mutual fossil content can now be correlated accurately by means of the composite standard. In this study, the software program *Graphcor 3.0* (Hood, 1998) was used.

CORRELATION OF THE STUDIED SECTIONS

The raw data on which the graphic correlation is based are available on request.The composite section at Bou Tchrafine was chosen as the regional composite reference section. Although this section is condensed and shows some hiatuses it is still the best-studied section from the set of sections available for this graphic correlation project. The bases and tops of the conodont taxa occurring in the Bou Tchrafine section are given in CSU in the Appendix listing all the conodont taxa mentioned in the paper. The nine remaining sections were correlated with the standard reference section in the following order: Hamer El Khdad South, Jbel El Atrous II, Hassi Nebch, Hassi Oum El Hadej, Jbel Bou Ifarherioun, Bou Terga, Jbel Amessoui, Ait ou Amar and Achguig. The lines of correlation (LOC) stabilised after four correlation rounds. For the LOC, a multi-segment line was preferred over a single-segment line because with the lithologies found in this region (alternating limestones and shales in some sections, massive limestone in others), correlations based on single-segment lines would result in artificial overlap of the conodont ranges. The three most important graphs (Figs. 6–8) are considered here.

JBEL EL ATROUS II SECTION (FIG 6)

The fourth round yielded a partly segmented but well-constrained line of correlation that intersects the first appearance of *Skeletognathus norrisi*, *Ancyrodella curvata* late form, *Palmatolepis kireevae*, *Ancyrognathus coeni* and *Ancyrodella alata*. The FADs of *Icriodus alternatus alternatus* and *Palmatolepis bogartensis* fall to the right of the LOC and will have as consequence an adjustment of the FAD in the CS.

HAMER EL KHDAD SOUTH SECTION (FIG. 7)

In this section the long error boxes indicate the lack of conodont samples in the middle part of the sequence. The LOC is well constrained in a few points and shows a horizontal terrace at level 1.8 m in the section, indicating that the base of the Frasnian is missing. The line of correlation passes through the

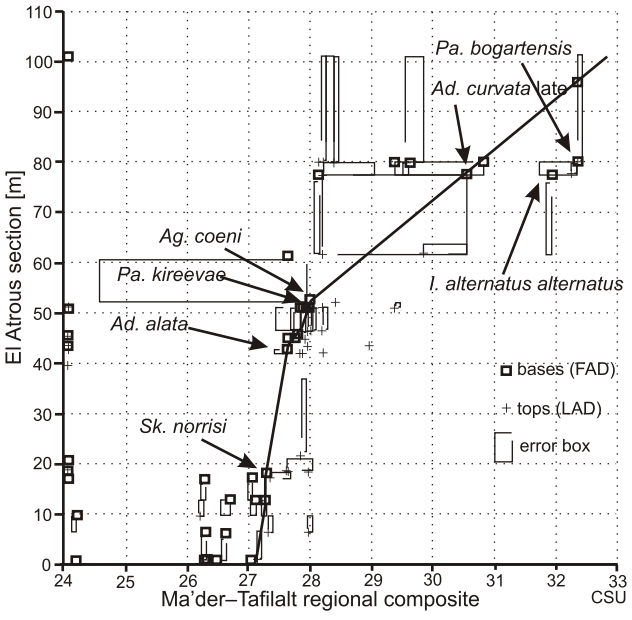

Fig. 6. Graphic correlation of the Jbel El Atrous II section and the Ma'der–Tafilalt regional composite standard

CSU — composite standard units

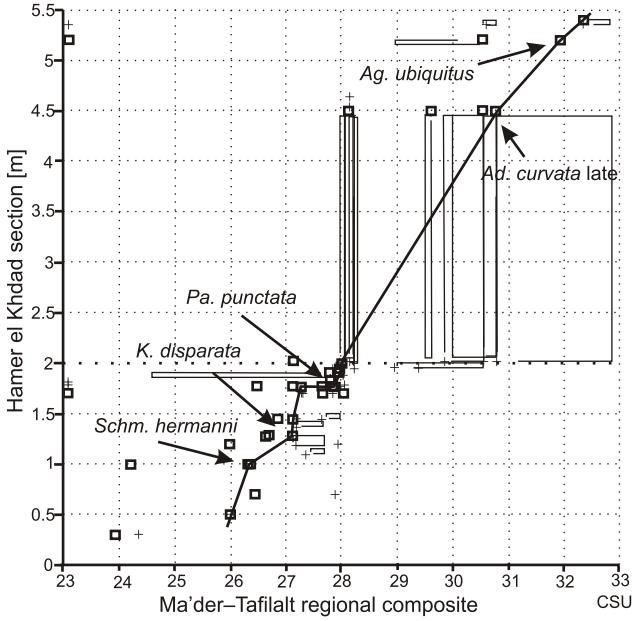

Fig. 7. Graphic correlation of the Hamer El Khdad South section and the Ma'der–Tafilalt regional composite standard

Symbols as in Figure 6

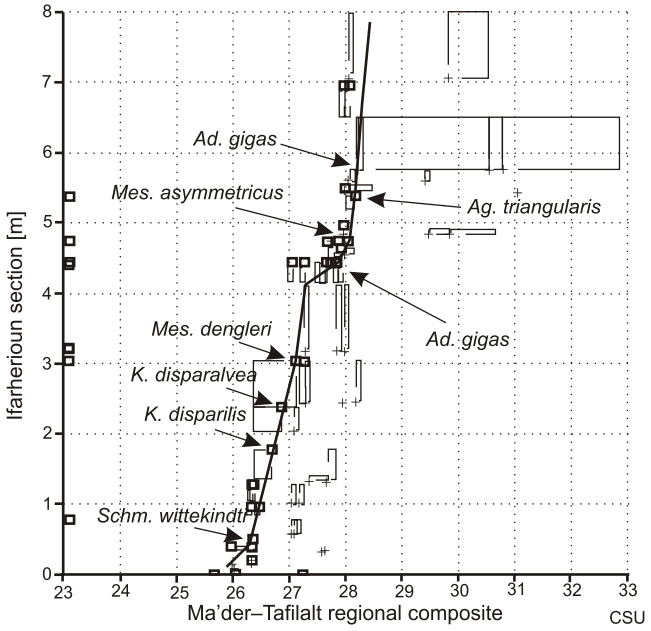

Fig. 8. Graphic correlation of the Jbel Bou Ifarherioun section with the Ma'der–Tafilalt regional composite standard

Symbols as in Figure 6

first occurrences of *Schmidtognathus hermanni*, *Klapperina disparata*, *Palmatolepis punctata*, *Ancyrodella curvata* late form and *Ancyrognathus ubiquitus*.

JBEL BOU IFARHERIOUN SECTION (FIG. 8)

In this graph the LOC was positioned, in places, by splitting the tops and bases of the error boxes. In parts of the graphs no correlation points are available and therefore several positions

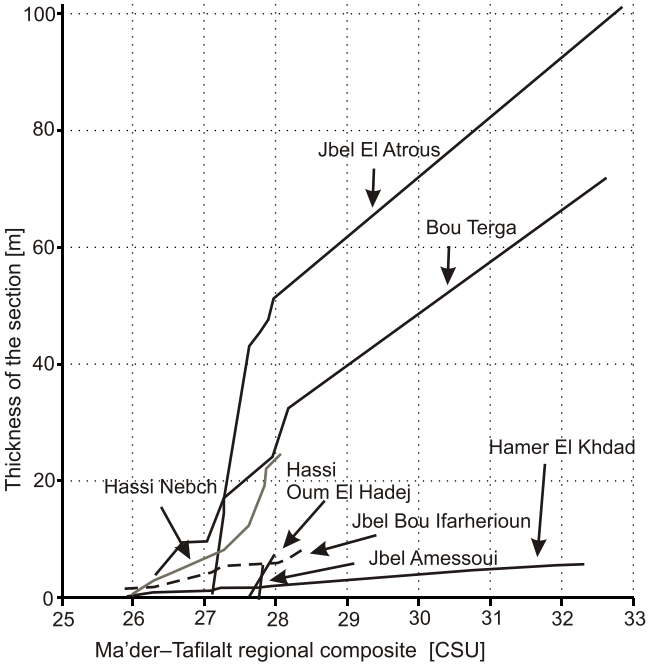

Fig. 9. Stratigraphic nomograph of the different sections

of the LOC are possible (e.g. between 3 and 4.5 m). The LOC intersects with the first occurrences of *Schmidtognathus wittekindti*, *Klapperina disparilis*, *Klapperina disparalvea*, *Mesotaxis dengleri*, *Ancyrodella gigas*, *Mesotaxis asymmetricus* and *Ancyrognathus triangularis*.

RESULTS

STRATIGRAPHIC NOMOGRAPH (FIG. 9)

The stratigraphic nomograph shows the LOCs of all correlated sections superimposed. The X-axis is the relative time scale; the vertical axis is scaled in metres. This display allows comparison of the sediment accumulation rates in the different sections and makes it easy to see a stratigraphic alignment of horizontal terraces in the LOCs. In the case of the Eastern Anti-Atlas there is no alignment of terraces but most of the LOCs show a change in the inclination of the line around the base of the Frasnian (CSU 27.33). Some show a steeper line others a less steep line compared to the regional composite reference section (Bou Tchrafine) indicating different degrees of condensation of the deposits near the base of the Frasnian.

CORRELATION OF THE DIFFERENT SECTIONS (FIGS. 10 AND 11)

The CSU scale of the regional composite reference section can be reprojected onto the sections through the LOCs of the correlation graphs. These CSU now allow a high-resolution correlation between the sections; even between sections that did not have enough data in common to correlate them amongst each other in the traditional two-by-two correlation. The CSU correlations should be evaluated in the light of the corresponding graphic correlation plots because the latter give information about the reliability/accuracy of the line of

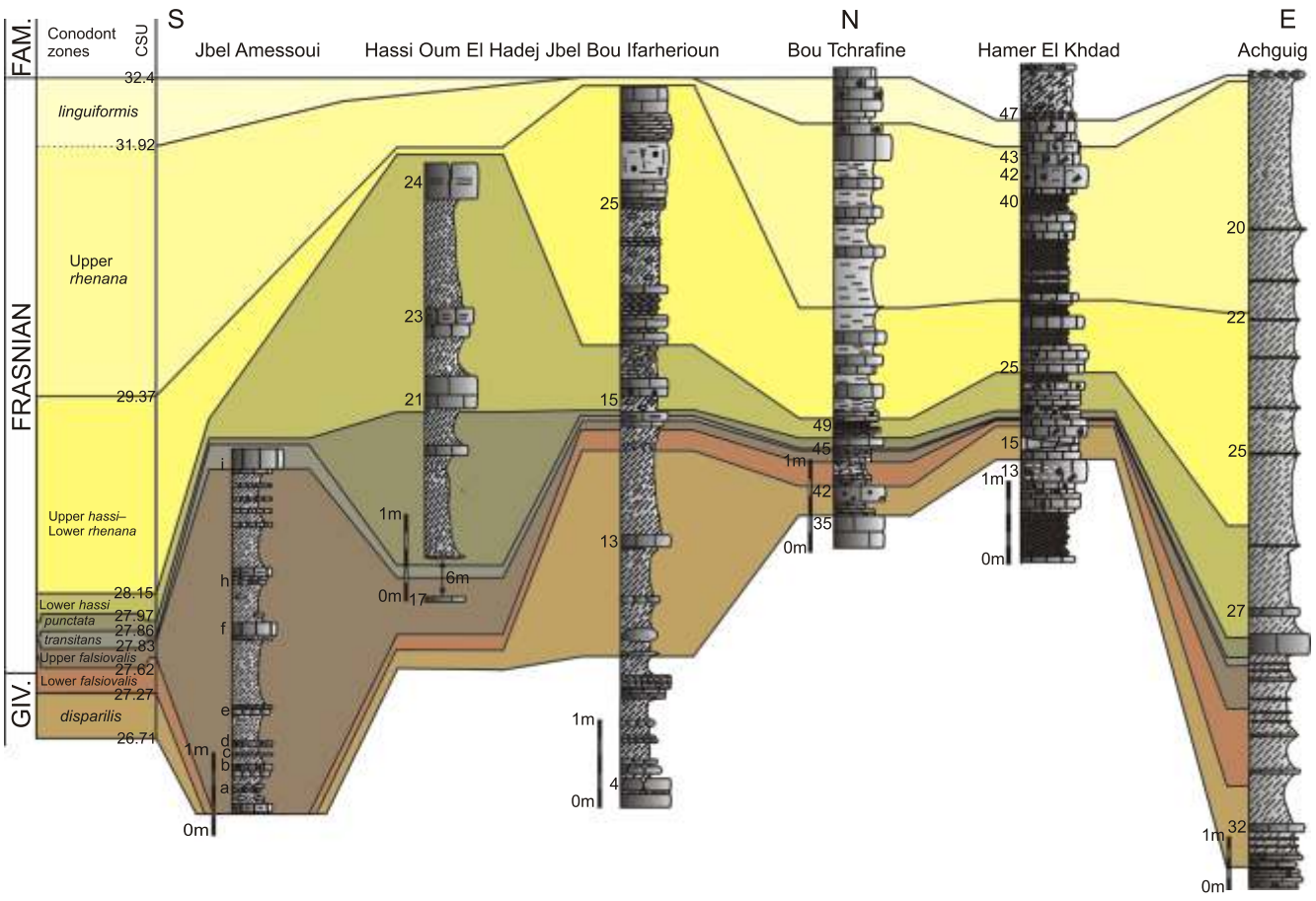

Fig. 10. Correlation of the upper Givetian-Frasnian sections of the Tafilalt Platform and Tafilalt Basin in south to north and to east direction, based on the results of the graphic correlation

Explanations as in Figures 2, 3 and 4; a few sample numbers are indicated next to the columns

correlation and thus the correlation of certain levels in the stratigraphic columns. The accurracy is indicated by the constraint of the LOC in that point on the graph and by the size of the error boxes of the correlation points. Figure 10 shows the correlation results between the sections of the Tafilalt Platform and Tafilalt Basin from the southern margin of the platform (Jbel Amessoui) to the north with more condensed limestone sedimentation (Bou Tchrafine) and to the east with thicker shaly intervals (Achguig). Figure 11 shows the correlation results between the sections from the Ma'der Platform in the west (Bou Terga) to the Tafilalt Platform (Jbel El Atrous) and Tafilalt Basin (Hassi Nebch) in the east.

The correlation of the sections shows very thin deposits representing the lower part of the Frasnian (especially the deposits of the *transitans* Zone) in the whole area (and especially in the Bou Tchrafine and Hamer El Khdad sections), thickening somewhat in the Ma'der and Tafilalt basins. The upper part of the Frasnian is characterized by thicker and more shaly intervals (except in the Hamar El Khdad section) thickening regularly in eastern direction (Achguig section) and in southwestern direction (Bou Terga section).

UPPER GIVETIAN–FRASNIAN ANTI–ATLAS CONODONT REGIONAL COMPOSITE AND CONODONT ZONES (FIG. 12)

The range charts given in Figure 12 are the visualisation of the Regional Composite database obtained after four graphic correlation rounds. The stratigraphic ranges of eighty-five conodont taxa have been assembled during this correlation project and positioned into the chronostratigraphic framework of composite standard units (CSU). The Frasnian of the Eastern Anti-Atlas can be subdivided into 501 CSU (27.33 – 32.34). Also the standard conodont zonation (Ziegler and Sandberg, 1990) can be aligned to the CSU framework. The conodont zones that can be positioned relative to the graphic correlation composite are: *hermanni* Zone (first occurrence of *Schmidtognathus hermanni* at CSU 26.3), *disparilis* Zone (first occurrence of *Klapperina disparilis* at CSU 26.71), Lower and Upper *falsiovalis* zones (respectively first occurrence of *Mesotaxis falsiovalis* at CSU 27.27 and first occurrence of *Mesotaxis asymmetricus* at CSU 27.62), *transitans* Zone (first occurrence of *Palmatolepis transitans* at CSU 27.83), *punctata* Zone (first occurrence of *Palmatolepis punctata* at CSU 27.86),

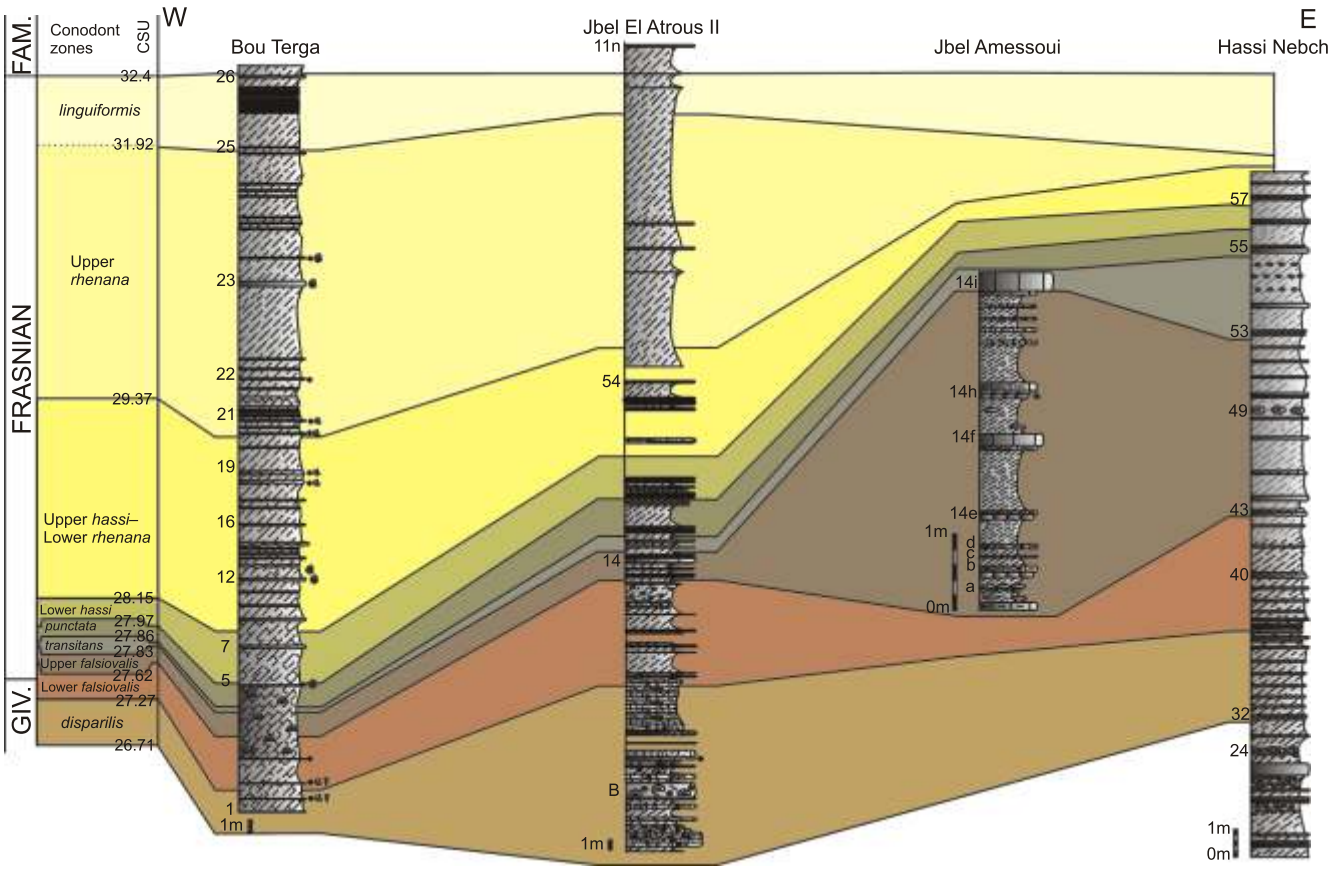

Fig. 11. Correlation of the upper Givetian-Frasnian sections of the Ma'der Basin, the Tafilalt Platform and Tafilalt Basin, in west to east direction, based on the results of the graphic correlation

Other explanations as in Figures 2, 3, 4 and 10

Lower *hassi* Zone (first occurrence of *Ancyrodella curvata* early form and *Ozarkodina trepta* at CSU 27.97), an interval ranging from the base of the Upper *hassi* Zone to the base of the Upper *rhenana* Zone (first occurrence of *Ancyrognathus triangularis* at CSU 28.15), Upper *rhenana* Zone (first occurrence of *Ancyrognathus asymmetricus* at CSU 29.37) and *linguiformis* Zone (first occurrence of *Ancyrognathus ubiquitus* CSU 31.92). The *jamieae* and Lower *rhenana* Zones cannot be placed since the defining taxa for those zones have not been found. The corresponding Montagne Noire zonation (Klapper and Becker 1999) is indicated on the figures by MN numbers. The bases of the first five zones are easily positioned. The base of MN6 (indicated by the first occurrence of *Ancyrognathus primus*) situated one CSU below the first occurrence of *Ozarkodina nonaginta* that indicates the base of MN7 is situated only one CSU higher than the base of MN6. The base of MN10 coincides with the base of the Upper *hassi* Zone here, which could indicate that the lower part of this zone is missing. The base of MN12 is here situated in the Upper *rhenana* Zone.

CORRELATION WITH THE FRASNIAN COMPOSITE STANDARD (FIG. 13)

The results of this graphic correlation project have been compared and correlated with the conodont Composite Standard of the Frasnian (Klapper, 1997; Gouwy and Bultynck, 2000).

Three horizontal segments (terraces) can be recognized in the line of correlation. One terrace is found at the level 27.6 of the Anti-Atlas regional composite indicating that deposits of the lower part of the Frasnian (upper part of the Lower *falsiovalis* Zone) are missing. A second terrace is found at level 28.1 of the Anti-Atlas regional composite to which deposits of the upper part of the Upper *hassi* Zone, the complete *jamieae* Zone and the lower part of the Lower *rhenana* Zone (MN11) would correspond. A third one is located at 28.9 of the Anti-Atlas regional composite indicating the lack of the lower part of the Lower *rhenana* Zone (lower part of MN12).

CONCLUSIONS

The graphic correlation of ten sections of the upper Givetian-Frasnian of the Eastern Anti-Atlas (Morocco) allows the development of a regional composite reference section that integrates the ranges of 85 conodont taxa. It provides the best possible stratigraphic resolution for the Frasnian of this region, even though the sections and conodont data are not of high quality because of sedimentary gaps and condensed intervals. The Frasnian of the Eastern Anti-Atlas is subdivided into 501 CSU (centimetre scale of the Bou Tchrafine reference section). Correlation with the CS of the Frasnian (Gouwy and Bultynck, 2000) shows that the upper part of the Upper *hassi* Zone, the

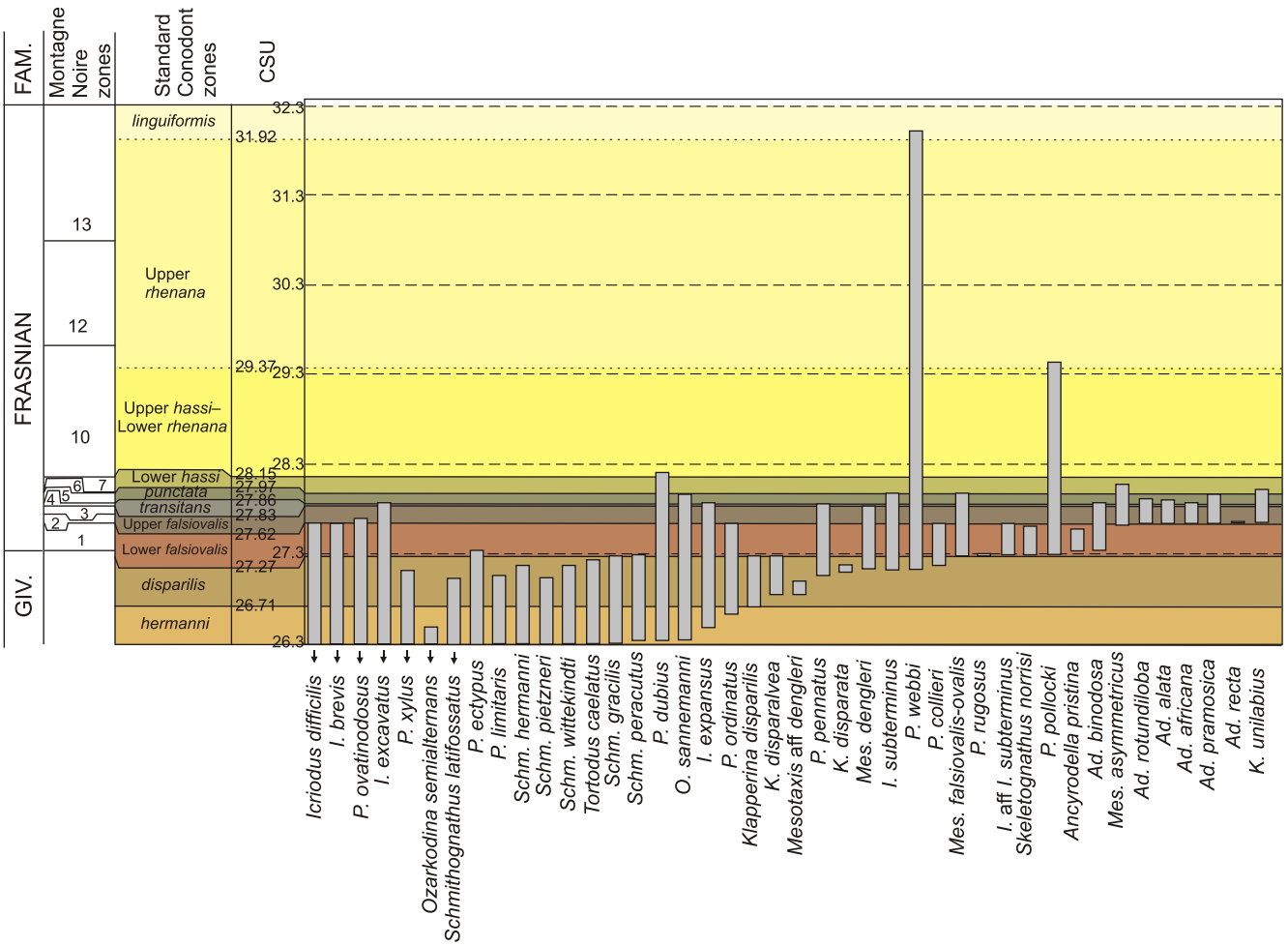

Fig. 12. Upper Givetian-Frasnian composite standard conodont ranges of the Ma'der–Tafilalt region; the *jamieae*

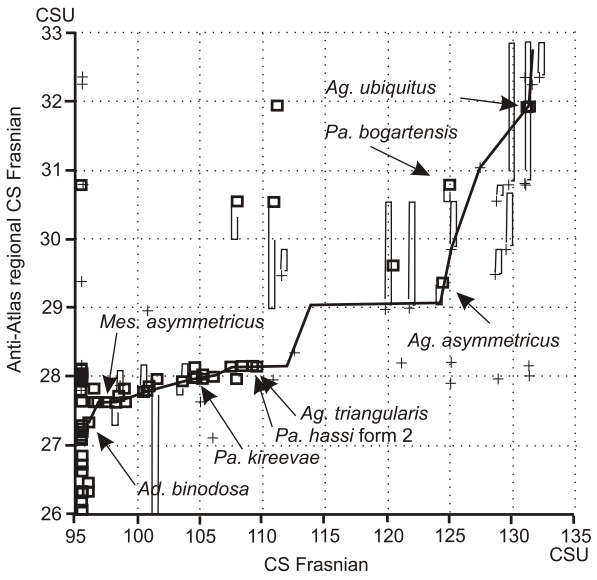

Fig. 13. Graphic correlation between the Ma'der–Tafilalt regional reference composite and the composite standard of the Frasnian (Gouwy and Bultynck, 2000)

Symbols as in Figure 6

jamieae Zone and the lower part of the Lower *rhenana* Zone are not found based on the available data. Because of the sedimentary gaps, condensed parts and barren intervals of the sections in the Eastern Anti-Atlas, these data have not been added to the CS of the Frasnian (Gouwy and Bultynck, 2000).

Acknowledgments. The late H. Hollard introduced one of the co-authors (P. B.) to the sections studied herein. The subsequent field-work has been partly carried out with L. Jacobs, P. Sartenaer, O. H. Walliser and the late W. Ziegler. B. Kaufmann and W. T. Kirchgasser thoroughly reviewed the manuscript. We owe many thanks to all for their contributions and comments.

Special thanks are due to M. Bensaid and M. Dahmani for the logistic assistance during the field-work received from the Direction des Mines et de la Géologie (Rabat).

J. Haydukiewicz contributions were made as part of an exchange programme between the University of Wrocław and the Katholieke Universiteit Leuven.

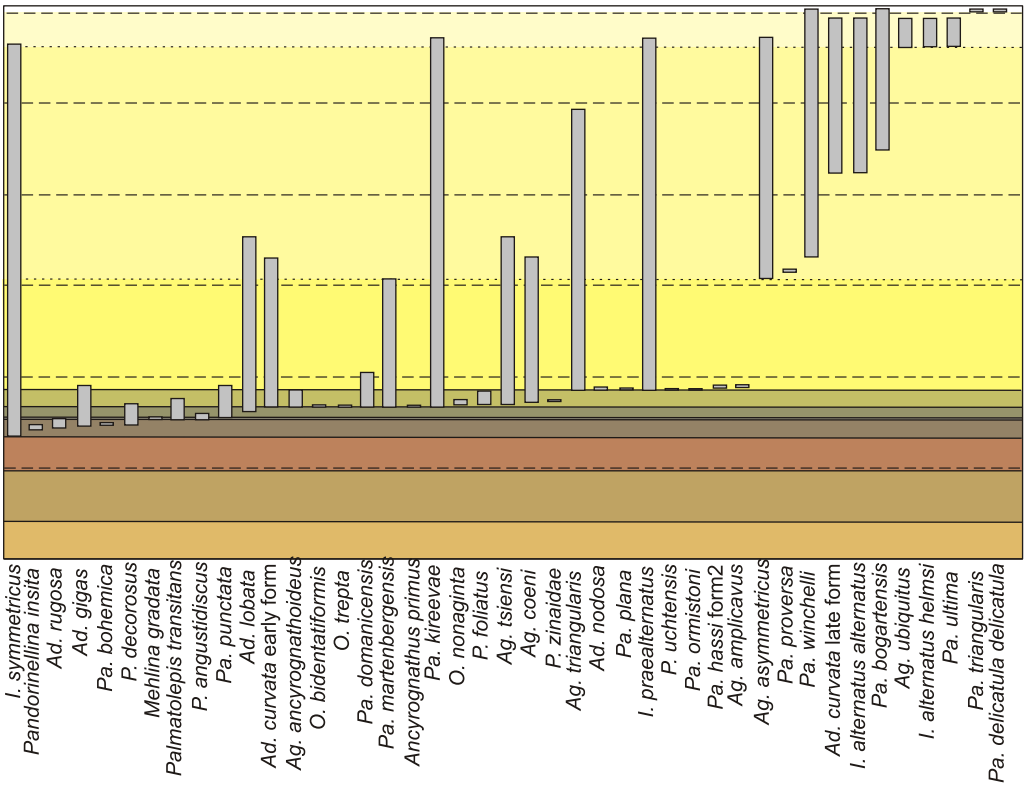

and Lower *rhenana* zones are not recognized in this region due to the lack of the diagnostic species of the zones

REFERENCES

BECKER R. T. and HOUSE M. R. (2000) — Late Givetian and Frasnian ammonoid succession at Bou Tchrafine (Anti-Atlas, Southern Morocco). Notes et Mém. Serv. Géol. Maroc, **399**: 27–36.

BELKA Z., KLUG C., KAUFMANN B., KORN D., DÖRING S., FEIST R. and WENDT J. (1999) — Devonian conodont and ammonoid succession of the eastern Tafilalt (Ouidane Chebbi section), Anti-Atlas, Morocco. Acta Geol. Pol., **49** (1): 1–23.

BENSAID M. (1972) — Untersuchungen über Goniatiten an der Grenze Mittel/Ober-Devon Süd-Marokkos. MS, Univ. of Bonn.

BENSAID M. (1974) — Etude sur des Goniatites a la limite du Devonien Moyen et Supérieure, du Sud Marocain. Notes Serv. Géol. Maroc, **36** (264): 81–140.

BENSAID M., BULTYNCK P., SARTENAER P., WALLISER O. H. and ZIEGLER W. (1985) — The Givetian-Frasnian Boundary in pre-Sahara Morocco. Courier Forsch.-Inst. Senckenberg, **75**: 287–300.

BULTYNCK P. (1986) — Accuracy and reliability of conodont zones: the *Polygnathus asymmetricus* "zone" and the Givetian-Frasnian boundary. Bull. Inst. Roy. Sc. Nat. Belg., Sc. de la Terre, **56**: 269–280.

BULTYNCK P. (1987) — Pelagic and neritic conodont successions from the Givetian of the pre-Sahara Morocco and the Ardennes. Bull. Inst. Roy. Sc. Nat. Belg. , Sc. de la Terre, **57**: 149–181.

BULTYNCK P., HELSEN S. and HAYDUCKIEWICH J. (1998) — Conodont succession and biofacies in upper Frasnian formations (Devonian) from the southern and central parts of the Dinant Synclinorium (Belgium) — (Timing of facies shifting and correlations with late Frasnian events). Bull. Inst. Roy. Sc. Nat. Belg., Sc. de la Terre, **68**: 25–75.

BULTYNCK P. and HOLLARD H. (1980) — Distribution comparée de Conodontes et Goniatites dévoniens des plaines du Dra, du Ma'der et du Tafilalt (Maroc). Aardkundige Med., **1**: 7–77.

BULTYNCK P. and JACOBS L. (1981) — Conodontes et sédimentologie des couches de passage du Givetien au Frasnien dans le nord du Tafilalt et dans le Ma'der (Maroc présaharien). Bull. Inst. Roy. Sc. Nat. Belg., **53** (2): 1–24.

BULTYNCK P. and WALLISER O. H. (2000*a*) — Emsian to Middle Frasnian sections in the northern Tafilalt. Notes et Mém. Serv. Géol. Maroc, **399**: 11–20.

BULTYNCK P. and WALLISER O. H. (2000*b*) — Devonian Boundaries in the Moroccan Anti-Atlas. In: Subcommission on Devonian Stratigraphy. Recognition of Devonian Series and stage boundaries in geological areas (ed. P. Bultynck). Courier Forsch.-Inst. Senckenberg, **225**: 211–226.

COEN-AUBERT M. (2002) — Nouvelles espèces du genre *Phillipsastrea* d' Orbigny, 1849 prés de la limite Givetien-Frasnien dans le Tafilalt et le Ma'der au Maroc et notes sur des types espagnols. Coral Res. Bull., **7**: 21–37.

GOUWY S. and BULTYNCK P. (2000) — Graphic correlation of Frasnian sections (Upper Devonian) in the Ardennes, Belgium. Bull. Inst. Roy. Sc. Nat. Belg., Sc. de la Terre, **70**: 25–52.

GOUWY S. and BULTYNCK P. (2002) — Graphic correlation of Middle Devonian sections in the Ardenne region (Belgium) and the Mader-Tafilalt (Morocco): development of a Middle Devonian composite standard. Aardk. Med., **12**: 105–108.

HOLLARD H. (1974) — Recherches sur la stratigraphie des Formations du Dévonien Moyen, de l'Emsien Supérieur au Frasnien, dans le Sud du Tafilalt et dans le Ma'der (Anti-Atlas oriental). Notes Serv. Géol. Maroc, **36** (264): 7–68.

HOOD K. C. (1998) — GraphCor, Interactive Graphic Correlation software, version 3.0, Houston.

HUDDLE J. W. assisted by REPETSKI J. E. (1981) — Conodonts from the Genesee Formation in western New York. Geol. Surv. Prof. Paper, **1032-B**.

KHALYMBADZHA V. G. and CHERNYSHEVA N. G. (1970) — Conodont genus *Ancyrodella* from Devonian deposits of the Volga–Kamsky area and their stratigraphic significance. In: Biostratigraphy and palaeontology of Palaeozoic deposits of the eastern Russian Platform and western pre-Urals (eds. A. B. Cus *et al.*). Kazan Univ., **1**: 81–103.

KAUFMANN B. (1998) — Facies, stratigraphy and diagenesis of Middle Devonian reef and mud-mounds in the Mader (eastern Anti-Atlas, Morocco). Acta Geol. Pol., **48** (1):43–106.

KLAPPER G. (1971) — Sequence within the conodont genus *Polygnathus* in the New York Middle Devonian. Geol. Palaeont., **5**: 59–79.

KLAPPER G. (1973) — *Polygnathus dubius* Hinde, 1879. In: Catalogue of conodonts (ed. W. Ziegler), **1**: 353–354.

KLAPPER G. (1985) — Sequence in conodont genus *Ancyrodella* in Lower *asymmetricus* Zone (earliest Frasnian, Upper Devonian) of the Montagne Noire, France. Palaeontograph. Abt. A, **188** (1–3): 19–34.

KLAPPER G. (1989) — The Montagne Noire Frasnian (Upper Devonian) conodont succession. In: Devonian of the world (eds. N. J. McMillan, A. F. Emmy and D. J. Glass). Can. Soc. Petrol. Geol. Mem., **14** (3): 449–468.

KLAPPER G. (1990) — Frasnian species of the Late Devonian conodont genus *Ancyrognathus*. J. Paleont., **64** (6): 998–1025.

KLAPPER G. (1997) — Graphic correlation of Frasnian (Upper Devonian) sequences in Montagne Noire, France, and Western Canada. GSA Spec. Pap.**,** **321**: 113–129.

KLAPPER G. and BECKER R. T. (1999) — Comparison of Frasnian (Upper Devonian) Conodont Zonations. Boll. Soc. Pal. It., **37**: 339–348.

KLAPPER G., KIRCHGASSER W. T. and BAESEMANN J. F. (1995) — Graphic correlation of a Frasnian (Upper Devonian) Composite Standard. In: Graphic correlation (eds. K. O. Mann, H. R. Lane and P. A. Scholle). SEPM Spec. Publ., **53**: 177–185.

KLAPPER G., PHILIP G. M. and JACKSON J. H. (1970) — Revision of the *Polygnathus varcus* group (Conodonta, Middle Devonian). N. Jb. Geol. Paläont. Mh., **11** : 650–667.

KLAPPER G., UYENO T. T., ARMSTRONG D. K. and TELFORD P. G. (2004) — Conodonts of the Williams Island and Long Rapids formations (Upper Devonian, Frasnian-Famennian) of the Onakawana B drillhole, Moose River Basin, northern Ontario, with a revision of the lower Famennian species. J. Paleont., **78** (2): 371–387.

MASSA D. (1965) — Observations sur les séries Siluro-Dévoniennes des confins Algéro-Marocains du Sud. Notes et Mém. Comp. Française Pétr., **8**.

MÜLLER K. J. and BENSAID M. (1969) — Devonian conodonts from Morocco. In: Proc. III African Micropal. Colloq., Cairo, March 4–10, 1968 (eds. R. Said, J. B. Beckmann, M. A. Ghorab, S. El Ansary, C. Viotti and M. T. Kerdany): 523–534.

NORRIS A. W. and UYENO T. T. (1983) — Biostratigraphy and palaeontology of Middle–Upper Devonian boundary beds, Gypsum Cliffs area, northeastern Alberta. Geol. Surv. Canada Bull., **313**.

NORRIS A. W., UYENO T. T. and McCABE H. R. (1982) — Devonian rocks of the Lake Winnipegosis-Lake Manitoba outcrop belt, Manitoba. Geol. Surv. Canada Mem., **392**, and Manitoba Miner. Resour. Publ., **771**.

SANDBERG C. A., ZIEGLER W., DREESEN R. and BUTLER J. L. (1988) — Late Frasnian mass extinctions: conodont event stratigraphy, global changes, and possible causes. Courier Forsch.-Inst. Senckenberg, **102**: 263–307.

SCOTESE C. R. (2004) — Paleomap project. www. scotese. com

SHAW A. B. (1964) — Time in stratigraphy. New York, McGrawhill.

UYENO T. T. (1967) — Conodont zonation, Waterways Formation (Upper Devonian), northeastern and central Alberta. Geol. Surv. Canada Pap., **67** (30).

WENDT J. (1985) — Disintegration of the continental margin of northwestern Gondwana, Late Devonian of the eastern Anti-Atlas (Morocco). Geology, **13**: 815–818.

WENDT J., AIGNER T. and NEUGEBAUER J. — Cephalopod limestone deposition on a shallow pelagic ridge: the Tafilalt Platform (upper Devonian, eastern Anti-Atlas, Morocco). Sedimentology, **31**: 601–625.

ZIEGLER W. (1966) — Eine Verfeinerung der Conodontengliederung an der Grenze Mittel-/ Oberdevon. Fortschr. Geol. Rheinld. U. Westf., **9**: 647–676.

ZIEGLER W. and KLAPPER G. (1982) — The *disparilis* conodont zone, the proposed level for the Middle–Upper Devonian boundary. Courier Forsch.-Inst. Senckenberg, **55**: 463–492.

ZIEGLER W., OVNATANOVA N. and KONONOVA L. (2000) — Devonian Polygnathids from the Frasnian of the Rheinisches Schiefergebirge, Germany, and the Russian Platform. Senckenbergiana lethaea, **80** (2): 593–645.

ZIEGLER W. and SANDBERG C. A. (1990) — The Late Devonian standard conodont zonation. Courier Forsch.-Inst. Senckenberg, **121**: 1–115.

APPENDIX

The Appendix includes all species/subspecies mentioned in the text and figures. Names of genera and species/subspecies are arranged alphabetically. The most important taxa are followed by either a reference to Figures 14 and 15 or by reference(s) to previous illustrations from Moroccan sections studied herein, or by both of them. Some of the taxa are briefly discussed. For taxa occurring in the Bou Tchrafine chosen herein as regional composite reference section, the bases (FAD) and tops (LAD) in CSU are given in brackets at the end of the respective taxon description information.

Ancyrodella africana Garcia-Lopez, 1981 (Fig. 15L); Bultynck and Hollard (1980, pl. 10, fig. 8, identified as *An. rotundiloba* aff. *An. alata*); (27.63–27.83).

Ancyrodella alata Glenister and Klapper, 1966 (Fig. 15I, J); Bultynck and Hollard (1980, pl. 9, figs. 15, 16, identified as *An. rotundiloba* aff. *An. alata*). The early and late forms distinguished by Klapper (1989) have been recognized; (early form 27.63–27.83, late form 27.83–27.85).

Ancyrodella binodosa Uyeno, 1967; ?Bultynck and Hollard (1980, pl. 10, figs. 4a, b); ?Bultynck and Jacobs (1981, pl. 9, figs. 3–5, 7, 8). Confident identifications of *An. binodosa* in the present paper refer only to adult specimens with a thick, circular- to oval-shaped platform with rounded margins and an upper surface ornamentation consisting of two large nodes on each side of the carina and occasionally a few incipient nodes (see Uyeno, 1967, pl. 1, figs. 4a, b). The pit is relatively large and cruciform. Such specimens occur in the section El Altrous II. Identifications as mentioned above are questioned because the upper surface ornamentation in the figured specimens is too much developed and these specimens may represent a late form of the species.

Ancyrodella curvata (Branson and Mehl, 1934) (Fig. 15P–T); Bultynck and Jacobs (1981, pl. 9, fig. 12, identified as *An. lobata*). The early and late forms distinguished by Klapper (1989) and the latest form of Bultynck *et al*. (1998) have been recognized; (early form 27.96–28.15).

Ancyrodella gigas Youngquist, 1947 (Fig. 15M, N); Bultynck and Jacobs (1981, pl. 9, figs. 9–11). The forms 1 and 3 of Klapper (1989) have been identified; (form 1: 27.83–28.20, form 3: 28.15–28.15).

Ancyrodella lobata Branson and Mehl, 1934 (Fig. 15O); Bultynck and Hollard (1980, pl.10, figs. 9–11); Bultynck and Jacobs (1981, pl. 9, fig. 13); (27.92–28.20).

Ancyrodella nodosa Ulrich and Bassler, 1926.

Ancyrodella pramosica Perri and Spalletta, 1981 (Fig. 15K); Bultynck and Jacobs (1981, pl. 10, figs. 10, 11, identified as *An. rotundiloba alata*); Bultynck (1986, pl. 1, figs. 10, 11, identified as *An. alata*); (27.63–27.87).

Ancyrodella pristina Khalymbadzha and Chernysheva, 1970; Bultynck and Jacobs (1981, pl. 8, figs. 1–14, pl. 9, figs 1, 2, 6, identified as *An. binodosa* forms alpha, beta, gamma). All these figured specimens are from one sample and are considered to represent an ontogenetic series of Pa elements of *An. pristina*. The specimens pl. 8, figs. 1–7 fall within the range of variation of the type specimens of *An. pristina/prima* figured by Khalymbadzha and Chernysheva (1970, pl. 1, figs. 1–8). The specimens of Bultynck and Jacobs (ibidem, pl. 8, figs. 11, 12) are considered as adult forms. Finally, *An. pristina* can be used either as a formal species name for the early form of *An. rotundiloba sensu* Klapper (1985) or as a subspecies of *An. rotundiloba*. Full-grown Pa elements can be separated from those of *An. rotundiloba* by the larger more oval-shaped, transversally developed cruciform pit and by the less dense upper surface ornamentation showing a pair of marked nodes in the anterior part of the platform, one on either side of the carina. The holotype of *An. soluta* Sandberg, Ziegler and Bultynck, 1989 is considered herein as an extreme form in the range of variation of *An. pristina*, close to *An. rotundiloba*; (aff. 27.35–27.35).

Ancyrodella recta Kralick, 1994; Bultynck and Jacobs (1981, pl. 10, fig. 9, identified as *An. rotundiloba rotundiloba*); Bultynck (1986, pl. 1, fig. 9, identified as *An. rotundiloba*); (27.63–27.63).

Ancyrodella rotundiloba (Bryant, 1921) (Fig. 15E–G); Bultynck and Hollard (1980, pl. 10, fig. 7); Bultynck and Jacobs (1981, pl. 10, figs. 1-8); Bultynck (1986, pl. 1, fig. 12); (27.63-27.63).

Ancyrodella rugosa Branson and Mehl, 1934 (Fig. 15H); (27.83–27.84).

Ancyrognathus amplicavus Klapper, Kuz'min and Ovnatanova, 1996; (28.15–28.15).

Ancyrognathus ancyrognathoideus (Ziegler, 1958); Bultynck and Hollard (1980, pl. 10, figs. 13, 15); (27.96–27.98).

Ancyrognathus asymmetricus (Ulrich and Bassler, 1926).

Ancyrognathus coeni Klapper, 1990; (28.15–28.15).

Ancyrognathus primus Ji, 1986; Bultynck and Hollard (1980, pl. 10, figs. 14, identified as *Polygnathus ancyrognathoideus*); (27.96–27.98).

Ancyrognathus triangularis Youngquist, 1945; (28.15–28.15).

Ancyrognathus tsiensi Mouravieff, 1982; diagnosis and description of Klapper (1990) are followed herein; *Ancyroides leonis* Sandberg, Ziegler and Dreesen, 1992 is considered as a junior synonym; (28.15–28.15).

Ancyrognathus ubiquitus Sandberg, Ziegler and Dreesen, 1988; (31.92–31.92).

Icriodus alternatus alternatus Branson and Mehl, 1934.

Icriodus alternatus helmsi Sandberg and Dreesen, 1984.

Icriodus brevis Stauffer, 1940; Bultynck (1987, pl. 6, figs. 9–12); (LAD 27.63).

Icriodus difficilis Ziegler and Klapper, 1976; Bultynck (1987, pl. 9, figs. 25, 26); (LAD 27.63).

Icriodus excavatus Weddige, 1984.

Icriodus expansus Branson and Mehl, 1938; Bultynck and Hollard (1980, pl. 8, fig. 23); (LAD 27.83).

Icriodus praealternatus Sandberg, Ziegler and Dreesen, 1992; (28.15–28.15).

Icriodus subterminus Youngquist, 1947; Bultynck and Hollard (1980, pl. 8, fig. 22); Bultynck (1986, pl. 2, figs. 13, 14); (27.29–27.30)

Icriodus* aff. *I. subterminus Youngquist, 1947; specimens identified in this way are similar to specimens of *Icriodus* cf. *I. subterminus* in Norris, Uyeno and McCabe (1982) and Norris and Uyeno (1983); (27.29–27.63);

Icriodus symmetricus Branson and Mehl, 1934; Bultynck and Hollard (1980, pl. 10, fig. 17); (27.63–28.20).

Klapperina disparalvea (Orr and Klapper, 1968); Bultynck and Hollard (1980, pl. 7, fig. 20); Bultynck and Jacobs (1981, pl. 7, fig. 13); (26.85–27.27).

Klapperina disparilis (Ziegler and Klapper, 1976); Bultynck and Jacobs (1981, pl. 7, fig. 14); (26.71–27.17).

Klapperina disparata (Ziegler and Klapper, 1982); Ziegler and Klapper (1982, pl. 2, figs. 6, 8, 10).

Klapperina unilabius (Huddle, 1981); Bultynck (1986, pl. 2, figs. 7, 10–12). The typical "L"-shaped pit of *Kl. unilabius* is raised above the level of the lower surface like it is the case in *Kl. disparilis* and in that way is clearly distinct from the pit in the *Mes. asymmetricus–ovalis–falsiovalis* group; (27.63–27.83).

Mehlina gradata Youngquist, 1945; (27.83–27.83).

Mesotaxis asymmetricus (Bischoff and Ziegler, 1957); Bultynck (1986, figs. 1, 2); (27.63–27.92).

Mesotaxis dengleri (Bischoff and Ziegler, 1957); Bultynck and Hollard (1980, pl. 8, figs. 2, 3); Bultynck and Jacobs (1981, pl. 7, figs. 3–9); (27.12–27.83).

Mesotaxis aff. ***Mes. dengleri*** (Bischoff and Ziegler, 1957); Bultynck and Jacobs (1981, pl. 7, figs. 1, 2, identified as *Polygnathus dengleri* alpha morphotype and alpha transitional to beta morphotype); (26.85–27.00).

Mesotaxis falsiovalis Sandberg, Ziegler and Bultynck, 1989; ***Mes. ovalis*** (Ziegler and Klapper, 1964); Bultynck and Jacobs (1981, pl. 7, figs. 12, 17, the latter identified as *Polygnathus asymmetricus asymmetricus*); Bultynck (1986, pl. 2, figs. 4–6, 8, 9); (27.27–27.92).

Ozarkodina bidentatiformis (Pham, 1979); (27.96–27.96).

Ozarkodina nonaginta Klapper, Kuz'min and Ovnatanova, 1996; (27.98–28.04).

Ozarkodina sannemanni (Bischoff and Ziegler, 1957); Bultynck and Hollard (1980, pl. 10, figs. 1–3, identified as *O.* aff. *O. sannemanni*); (27.17–27.96).

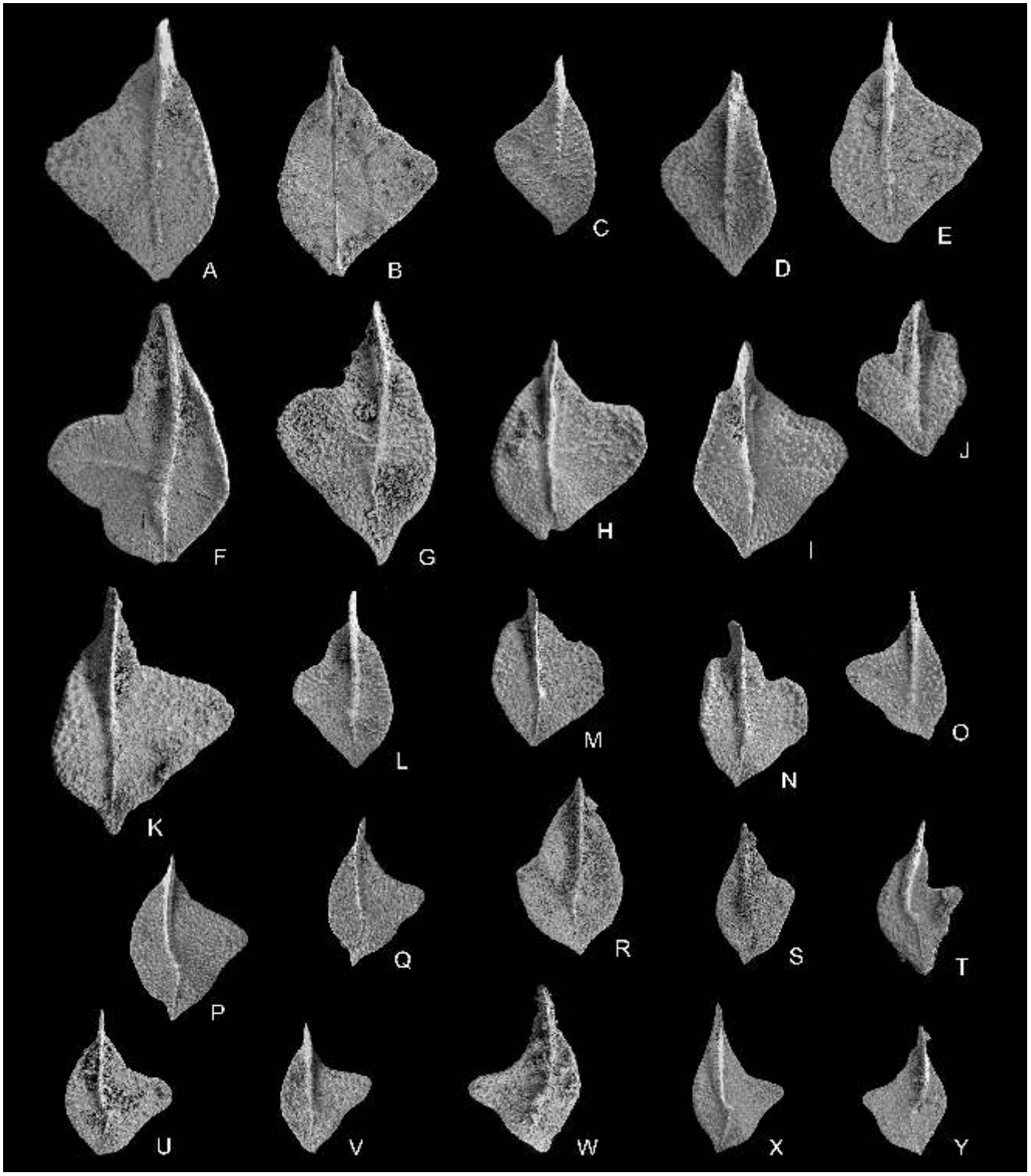

Fig. 14. *Palmatolepis* Pa elements

A–E — *Palmatolepis transitans* Müller, 1956: A, B — sample BT37bis (= base BT45), b4924, × 22, C — sample BT37bis, b4925, D — sample BE5a (= base BE5), b4926, E — sample EA11d, b4927; **F** — *Palmatolepis martenbergensis* Müller, 1956, sample BT47, b4928, × 22; **G, H** — *Palmatolepis punctata* (Hinde, 1879): G — sample BT48, b4929, × 22, H — sample EA32, b4930, × 22; **I, J —** *Palmatolepis bohemica* Klapper and Foster, 1993: I — sample EA32, b4931, J — sample If16, b4932; **K** — *Palmatolepis* n.sp. A, sample BE5b (= top BE), b4933, × 22; **L–N** — *Palmatolepis plana* Ziegler and Sandberg, 1990, sample BT38 (= BT51), b4934, b4935, b4936; **O–Q** — *Palmatolepis kireevae* Ovnatanova, 1976: O — sample BT38 (=BT51), b4937, P — sample EA32, b4938, Q — sample If16, b4939; **R, S** — *Palmatolepis domanicensis* Ovnatanova, 1976: R — sample BT47, b4940, S — sample TM912 (from approximately the same level as sample BE9), b4941; **T** — *Palmatolepis proversa* Ziegler, 1959, sample BE21, b4942; **U** — *Palmatolepis hassi* Müller and Müller, 1957 form 2 Klapper 1989, sample BT38 (= BT51), b4943; **V** — *Palmatolepis ormistoni* Klapper, Kuz'min and Ovnatanova, 1996, sample BT38 (= BT51), b4944, × 30; **W, X** — *Palmatolepis winchelli* (Stauffer, 1938): W — sample BE26, b4945, X — sample EA11m, b4946; **Y** — *Palmatolepis bogartensis* (Stauffer, 1938), sample BE26, b4947; all figures are upper views (except B, lower view), magnifications are approximately × 26 (unless otherwise stated); BT — Bou Tchrafine section, BE — Bou Terga section, EA — El Atrous II section, If — Ifarherioun section, TM samples were provided by the late Henri Hollard; all specimens are reposited at the Institut Royal des Sciences Naturelles de Belgique (Brussels) under catalogue numbers b4924–b4966

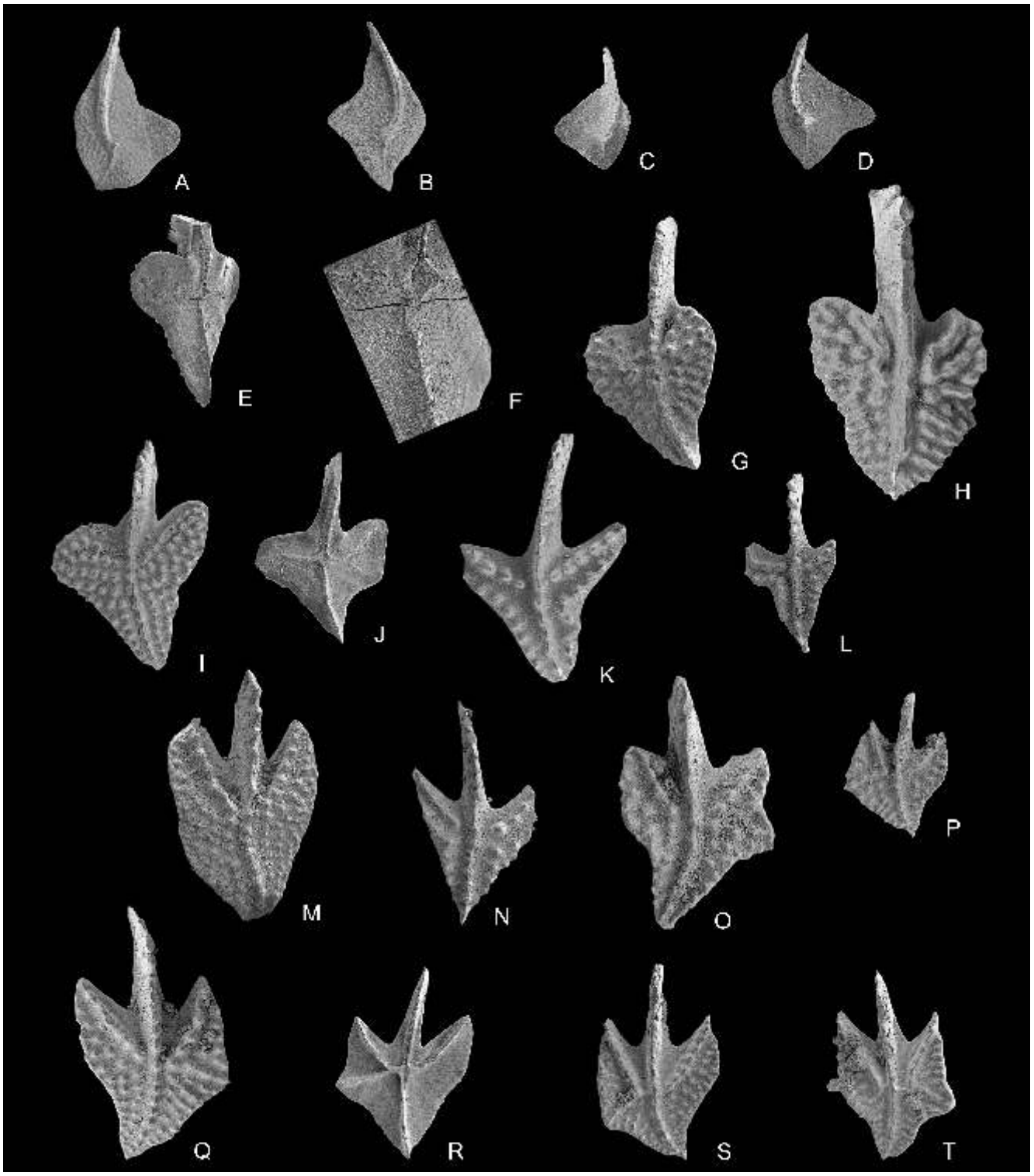

Fig. 15. *Palmatolepis* and *Ancyrodella* Pa elements

A — *Palmatolepis bogartensis* (Stauffer, 1938), sample EA11m, b4948, × 26; **B** — *Palmatolepis triangularis* Sanneman, 1955, sample EA11n, b4949, × 26; **C, D** — *Palmatolepis delicatula delicatula* Branson and Mehl, 1934, sample EA11n, b4950, b4951, × 26; **E–G** — *Ancyrodella rotundiloba* (Bryant, 1921), BT37bis (= base BT45), b4952, b4953: F — detail of E showing typical rhombic pit and without secondary keels (× 95); **H** — *Ancyrodella rugosa* Branson and Mehl, 1934 BT37bis(= base BT45), b4954; **I, J** — *Ancyrodella alata* Glenister and Klapper, 1966 late form of Klapper 1989, BT37bis (= base BT45), 4955, b4956; **K** — *Ancyrodella pramosica* Perri and Spalletta, 1981, sample BT37bis (= base BT45), b4957; **L** — *Ancyrodella africana* Garcia-Lopez, 1981, sample BT37bis (= base BT45), b4958; **M, N** — *Ancyrodella gigas* Youngquist, 1947: M — sample BT51, b4959, form 3 of Klapper, 1989, N — sample BT37bis (= base BT45), b4960, form 1 of Klapper, 1989; **O** — *Ancyrodella lobata* Branson and Mehl, 1934, sampleBE5a (= base BE5), b4961; **P–S** — *Ancyrodella curvata* (Branson and Mehl, 1934) early form of Klapper, 1989: P, S — sample BE21, b4962, b4965, Q, R — TM916 (from approximately the same level as sample BE12); **T** — *Ancyrodella curvata* (Branson and Mehl, 1934) late form of Klapper, 1989, sample BE21, b4966; all figures are upper views (except E, F, J and R, lower views), magnifications are approximately × 30 (unless otherwise stated), see also Figure 14 for explanations about sample numbers and catalogue numbers

Ozarkodina semialternans (Wirth, 1967); Bultynck and Hollard (1980, pl. 8, figs. 5, 6); (26.20–26.48).

Ozarkodina trepta (Ziegler, 1958); (27.96–28.00).

Pandorinellina insita (Stauffer, 1940); only one incomplete specimen has been found, in sample BT43; (27.27–27.27).

Palmatolepis bogartensis (Stauffer, 1938) (Fig. 14Y and Fig. 15 A); *Pa. bogartensis* is a senior synonym for *Pa. rotunda* Ziegler and Sandberg, 1990.

Palmatolepis bohemica Klapper and Foster, 1993 (Fig. 14I, J).

Palmatolepis delicatula delicatula Branson and Mehl, 1934 (Fig. 15C, D).

Palmatolepis domanicensis Ovanatanova, 1976 (Fig. 14R, S); (27.96–27.98).

Palmatolepis hassi Müller and Müller, 1957 form 2 Klapper, 1989 (Fig. 14U); (28.15–28.15).

Palmatolepis kireevae Ovnatanova, 1976 (Fig. 14O–Q); (27.96–28.15).

Palmatolepis martenbergensis Müller, 1956 (Fig. 14F); Bultynck and Hollard (1980, pl. 10, figs. 18, 19). *Pa. martenbergensis* is separated herein from *Pa. punctata* by the presence of a deep sinus anterior of the lobe and a clear sinus posterior of the lobe. In the holotype of *Pa. punctata* the sinus anterior of the lobe is shallow and there is almost no sinus posterior of the lobe; (27.96–28.20).

Palmatolepis ormistoni Klapper, Kuz'min and Ovnatanova, 1996 (Fig. 14V); (28.15–28.15).

Palmatolepis plana Ziegler and Sandberg, 1990 (Fig. 14L–N); (28.15–28.15).

Palmatolepis proversa Ziegler, 1959 (Fig. 14T).

Palmatolepis punctata (Hinde, 1879) (Fig. 14G, H); Bultynck and Jacobs (1981, pl. 7, fig. 15 only, identified as *Pa. transitans*, this specimen is very similar to the holotype of *Pa. punctata*); see also comments under *Pa. martenbergensis*; (27.86–28.06).

Palmatolepis transitans Müller, 1956 (Fig. 14A–E); Bultynck and Jacobs (1981, pl. 7, fig. 16 only); (27.83–28.06).

Palmatolepis triangularis Sannemann, 1955 (Fig. 15B).

Palmatolepis ultima Ziegler, 1959; Sandberg *et al*. (1988, pl. 1, figs. 1–4, identified as *Pa. praetriangularis* n.sp. Ziegler and Sandberg, same locality as Hamar El Khdad herein); *Pa. praetriangularis* is a junior synonym of *Pa. ultima* (see Klapper *et al*., 2004).

Palmatolepis winchelli (Stauffer, 1938) (Fig. 14W, X); *Pa. winchelli* is a senior synonym for *Pa. subrecta* Miller and Youngquist, 1947.

***Palmatolepis* n.sp. A** (Fig. 14K). The Pa element of *Pa.* n.sp. A has a wide, triangular platform; it is characterized by a prominent, broad laterally extending lobe; the anterior sharp lobe incision is into the first-fourths part of the platform, more or less perpendicular to the carina; the blade-carina is rectilinear and an incomplete secondary carina can be present; in adult specimens the central node is only slightly differentiated; the posterior outer platform margin is nearly straight; the posteriormost part of the platform is attenuating and pointed; in *Pa. punctata* the carina is slightly sigmoidal and there is only a shallow sinus in the anterior outer platform margin; *Pa.* n. sp. A occurs in the *transitans* and *punctata* zones; (27.83–27.83).

Polygnathus angustidiscus Youngquist, 1945; (27.83–27.83).

Polygnathus collieri Huddle, 1981; Bultynck (1986, pl. 1, fig. 8); (27.17–27.63).

Polygnathus decorosus Stauffer, 1938; in accordance with the diagnosis of Klapper, Philip and Jackson (1970); (27.29–28.06).

Polygnathus dubius Hinde, 1879; *sensu* Klapper (1973, pl. 1, fig. P); (26.72–28.20).

Polygnathus ectypus Huddle, 1934; Bultynck and Hollard (1980, pl. 9, figs. 13, 14, identified as *P. cristatus*); Bultynck and Jacobs (1981, pl. 7, figs. 10, 11, identified as *P. cristatus*); see discussion on *P. cristatus* and *P. ectypus* in Huddle, 1981; (26.30–27.35).

Polygnathus foliatus Bryant, 1921; *sensu* Ziegler *et al*. (2000, pl. 1, figs. 28, 29); (28.00–28.15).

Polygnathus limitaris Ziegler and Klapper, 1976; Bultynck and Hollard (1980, pl. 8, fig. 14); (26.30–27.05).

Polygnathus linguiformis linguiformis Hinde, 1879; (LAD 26.20).

Polygnathus ordinatus Bryant, 1921; Bultynck and Hollard (1980, pl. 8, fig. 18); (26.62–27.63).

Polygnathus ovatinodosus Ziegler and Klapper, 1976; Bultynck and Hollard (1980, pl. 8, figs. 10, 11); (26.30–27.17).

Polygnathus pennatus Hinde, 1879; Bultynck and Hollard (1980, pl. 8, fig. 21); Bultynck (1986, pl. 1, fig. 4); (27.05–27.63).

Polygnathus pollocki Druce, 1976; Bultynck (1986, pl. 1, figs. 1, 2); (27.29–27.43).

Polygnathus rugosus Huddle, 1934 *sensu* Ziegler, 1966; Bultynck (1986, pl. 1, fig. 13); (27.27–27.27).

Polygnathus uchtensis Ovnatanova and Kuz'min, 1991; (28.15–28.15).

Polygnathus webbi Stauffer, 1938; identification is based on the remarks in Klapper (1971).

Polygnathus xylus Stauffer, 1940; Bultynck (1987, pl. 8, figs. 22, 27); in accordance with the diagnosis of Klapper, Philip and Jackson (1970); (LAD 27.05).

Polygnathus zinaidae Kononova, Alekseev, Barskov and Reimers, 1996.

Schmidtognathus gracilis Klapper, 1980; Bultynck and Jacobs (1981, pl.7, figs. 4, 5).

Schmidtognathus hermanni Ziegler, 1966; Bultynck and Hollard (1980, pl. 9, figs. 9, 10); (26.30–26.48).

Schmidtognathus latifossatus Wirth, 1967; Bultynck and Hollard (1980, pl. 9, figs. 11, 12); (26.20–26.62).

Schmidtognathus peracutus (Bryant, 1921); Bultynck and Hollard (1980, pl. 8, fig. 24); (27.00–27.29).

Schmidtognathus pietzneri Ziegler, 1966; Bultynck and Hollard (1980, pl. 9, figs. 7, 8); (26.30–26.62).

Schmidtognathus wittekindti Ziegler, 1966; Bultynck and Hollard (1980, pl. 9, figs. 4, 5); (26.30–27.05).

Skeletognathus norrisi (Uyeno, 1967); Bultynck and Hollard (1980, pl. 8, fig. 12); Bultynck (1986, fig. 5); (27.29–27.61).

Tortodus caelatus (Bryant, 1921); Bultynck and Hollard (1980, pl. 8, figs. 1, 9, identified as *Polygnathus* aff. *P. beckmanni* and *P. beckmanni*); (24.20–26.20).